inorganics

MDPI

Article

Electronic Effects of the Substituents on Relaxometric and CEST Behaviour of Ln(III)-DOTA-Tetraanilides

Valeria Lagostina [1,2], Loredana Leone [1], Fabio Carniato [1], Giuseppe Digilio [1], Lorenzo Tei [1] and Mauro Botta [1,*]

[1] Dipartimento of Scienze e Innovazione Tecnologica, Università del Piemonte Orientale, Viale T. Michel 11, 15121 Alessandria, Italy; valeria.lagostina@unito.it (V.L.); loredana.leone@uniupo.it (L.L.); fabio.carniato@uniupo.it (F.C.); giuseppe.digilio@uniupo.it (G.D.); lorenzo.tei@uniupo.it (L.T.)

[2] Department of Chemistry, University of Torino, via Giuria 7, I-10125 Torino, Italy

* Correspondence: mauro.botta@uniupo.it; Tel.: +39-0131-360253

Received: 31 January 2019; Accepted: 11 March 2019; Published: 27 March 2019

Abstract: Three different 1,4,7,10-tetraazacyclododecane-1,4,7,10-tetraacetamide (DOTAM) derivatives bearing as amide *N*-substituents phenyl, *p*-methoxyphenyl and *p*-ethylbenzoate groups were synthesized and the ^{1}H and ^{17}O NMR relaxometric behaviour of the Gd(III)-chelates and chemical exchange saturation transfer (CEST) effect of the Eu(III) complexes were evaluated. The electronic properties of the substituents were shown to strongly influence the coordinated water exchange rate (k_{ex}), resulting in five times faster k_{ex} for the electron donating phenylmethoxy group compared to the electron withdrawing ethylbenzoate group.

Keywords: macrocyclic ligands; lanthanide complexes; relaxometry; CEST; electronic effects

1. Introduction

1,4,7,10-tetraazacyclododecane-1,4,7,10-tetraacetic acid (DOTA) and its derivatives have been thoroughly investigated in the last thirty years because of their widespread use as chelators for metal ions used as reporters in several imaging techniques such as magnetic resonance (MR), positron emission tomography (PET), single-photon emission computed tomography (SPECT) and fluorescence imaging [1,2]. The most significant properties of DOTA-like chelates are their remarkable thermodynamic stability and kinetic inertness towards both transmetallation reactions and acid-catalysed dissociation [3]. These properties coupled to the versatility of DOTA-like ligands towards several metal ions, from transition to lanthanide and actinide ions, have favoured the use of DOTA-based systems in a broad range of different applications. The primary use of DOTA-like ligands has been for the coordination of lanthanide ions, from Gd(III) for MRI applications [4,5] to Eu(III) and Tb(III) for fluorescence and Nd(III) for near infra-red imaging [6].

The tetraamide derivatives of DOTA form Ln(III) complexes bearing a positive charge (+3) with a very slow water exchange rate (k_{ex}), in the order of 60,000 s^{-1} at 298 K for GdDOTAM (DOTAM = 1,4,7,10-Tetrakis(carbamoylmethyl)-1,4,7,10-tetraazacyclododecane) [7]. This property limits the ability of the complex to increase the nuclear magnetic relaxation rate of the water protons, and therefore, the relaxivity of GdDOTAM-like complexes is typically quite low (in the range of 2–3 mM^{-1} s^{-1}). In particular, Gd-complexes with sterically hindered and hydrophobic substituents have a limited solvent accessible surface area and show the slowest water exchange rates [8]. In addition, the chemical nature of the counter-ion can influence the k_{ex} of such Gd-complexes, with faster values found for larger ions with a lower charge density such as iodine [9]. However, the long residence time of the coordinated water molecule ($\tau_M = 1/k_{ex}$) has allowed determining the rate of prototropic exchange in

basic media [10,11]. This acceleration of prototropic exchange, mainly caused by deprotonation of the bound water molecule, led to a remarkable increase in relaxivity at pH > 8 [12].

Notably, the studies on k_{ex} modulation on GdDOTA–tetraamide complexes paved the way for the development of paramagnetic chemical exchange saturation (PARACEST) agents, which can exploit both the protons of a slow exchanging metal-bound water molecule and the amide protons present on the ligand and in dynamic exchange with the solvent [13,14]. These protons have to be in the appropriate time regime of dynamic exchange with bulk water protons to be able to observe a CEST effect following saturation of the proton signal of the bound water or amides. Several studies have been reported on the effect of changing the substituents on the amide nitrogen to modulate the PARACEST effect of the Ln(III) complexes, especially for the development of responsive probes [15,16]. Moreover, a series of Dy^{3+} and Tm^{3+} para-substituted DOTA-tetraanilide complexes have been recently reported and tested for their ability to show pH responsive CEST effects. However, the poor solubility of many of the compounds limited the results obtained for these type of systems [17].

Data in the literature for Gd(III)-DOTA-tetraamide derivatives proved that electron-donating substituents are able to increase the electron density on Gd^{3+} ion through the coordinating amide arms, thus accelerating water exchange. On the contrary, electron-withdrawing functionalities operate in the opposite direction, decelerating water exchange [18]. In order to get more information on how the electronic properties of the ligand affect the water exchange process, three different DOTAM-like derivatives bearing in the structure for phenyl (L1), *p*-methoxyphenyl (L2) and *p*-ethylbenzoate (L3) groups were synthesized (Scheme 1) and their Ln(III) complexes (Scheme 2) studied in detail. In particular, the relationship that exists between the electronic properties of these substituents [19] and both the relaxometric behaviour of the Gd(III)-chelates and the CEST effect of the Eu(III) complexes were evaluated.

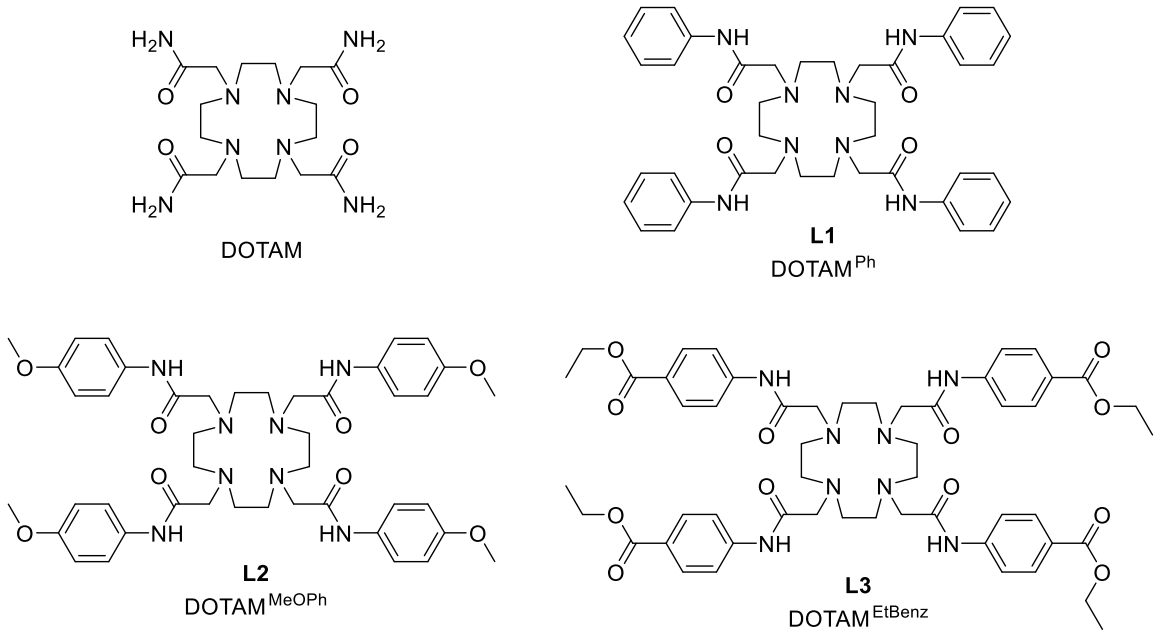

Scheme 1. 1,4,7,10-tetraazacyclododecane-1,4,7,10-tetraacetic acid (DOTA)-tetraamide ligands discussed in the text.

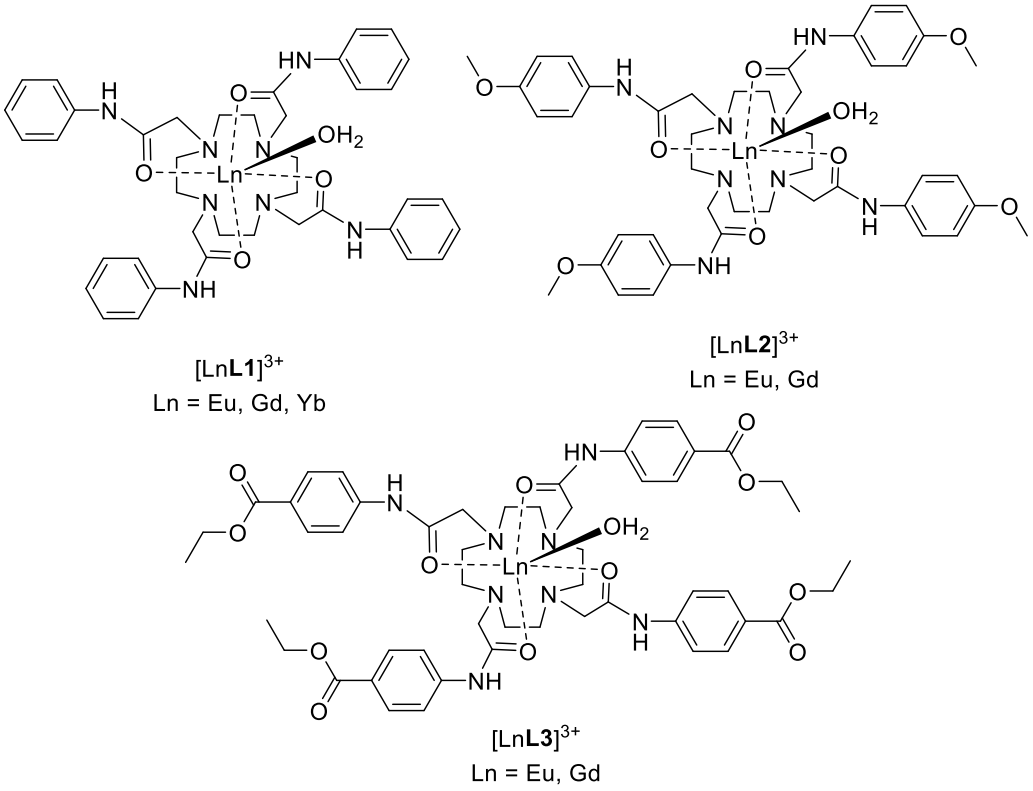

Scheme 2. Ln(III) complexes with ligands L1, L2 and L3.

2. Results and Discussion

2.1. Synthesis

The bromoacetamides used for the alkylation of cyclen were synthesized using a procedure slightly changed with respect to those already reported in the literature [17,20]. In particular, the aniline (and *p*-substituted aniline) and bromoacetylbromide were reacted under Schotten–Baumann conditions (NaOH 1 M and CH_2Cl_2 phases) in 75–80% yield. The tetra-substituted cyclens were obtained by refluxing for 24 h cyclen with 4.5 eq. of the appropriate electrophiles in acetonitrile in the presence of potassium carbonate. After this reaction time, the products precipitated from the acetonitrile solution were washed with water and obtained in ca. 60% yield. The Ln(III) complexes were then obtained by mixing the ligands, dissolved in a 1:1 dimethylformamide/H_2O solution, with an aqueous solution of the Ln–triflate heated at 50 °C for 36 h, followed by HPLC-MS analysis. Finally, to increase the water solubility of the complexes, the triflate anions were exchanged with chlorides by passing the complex through a Dowex ion-exchange resin.

2.2. Relaxometry

The longitudinal water proton relaxation rate in aqueous solution of the Gd(III) complexes was measured as a function of the applied magnetic field strength and temperature. The parameter relaxivity (r_1, mM^{-1} s^{-1}), which represents the increase of the relaxation rate of the solvent water protons in the presence of one millimolar solution of the metal ion, measures the relaxation efficiency of the paramagnetic complex. In the first step, the relaxivity value of the three complexes was measured as a function of pH in the range of 2–10, at 298 K and 20 MHz (Figure 1). The pH dependency has a behaviour rather typical of cationic Gd(III) chelates characterized by a markedly slow rate of exchange of the bound water molecule. The relaxivity remained unchanged in the pH range of about 2–8, assuming a very low value that was comparable to that of complexes with a hydration number equal to zero (q = 0). These r_1 values were consistent with the occurrence of an outer-sphere contribution

only. On the other hand, at basic pH values, the relaxivity increased dramatically, reaching up to values comparable to or greater than those of monohydrated complexes. In the case of GdL1 and GdL2, the observed increase was fully reversible and quite well understood. It arose from a prototropic exchange contribution catalysed by the addition in the solution of increasing amounts of [OH^-]. Under this condition, it was shown previously that k_{ex} was determined by the expression ($k_1 + k_2[OH^-]$), where k_1 refers to the exchange of the entire water molecule and k_2 accounts for the prototropic exchange. A strong enhancement of r_1 from pH 8 to pH 10 was observed also for GdL3, but in this case, the behaviour was not reversible, and it can be tentatively attributed to a modification of the chemical structure of the complex associated with the saponification of the ester groups (Figure 1).

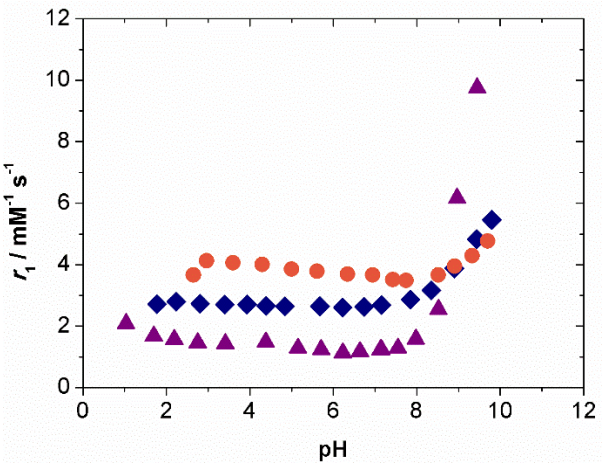

Figure 1. pH dependence of r_1 at 20 MHz and 298 K for aqueous solutions of GdL1 (♦ , 2.9 mM), GdL2 (•, 2.7 mM), and GdL3 (▲ , 1.8 mM).

The water exchange rate of the inner sphere water molecule (k_{ex}) in the three complexes was determined through the measurement and analysis of the temperature dependence of the ^{1}H relaxivity and ^{17}O NMR transverse relaxation rates and chemical shifts. The temperature dependence of r_1 (^{1}H-VT) represents a simple and effective way to obtain key information on the exchange regime of the coordinated water molecule(s). When the mean lifetime of coordinated water ($\tau_M = 1/k_{ex}$) does not limit r_1, as for most anionic and neutral Gd(III)-chelates, the longitudinal relativity decreases by increasing temperature, due to the increased value of the diffusion coefficient (D) of bulk water and the higher rate of molecular tumbling (shorter τ_R). The ^{1}H-VT profiles for GdL1–L3, measured in the range 278 to 345 K, showed a quite different trend (Figure 2). r_1 decreased from 278 to approximately 295 K, then it grew moderately up to about 330 K where it reached a maximum value in the case of GdL1 and GdL2. Unlike GdL1 and GdL2, the relaxivity of GdL3 continued to increase up to 345 K. This behaviour can be attributed to a residence lifetime of the inner sphere water long enough to make the inner sphere contribution (IS) to relaxivity negligible at intermediate or low temperatures. In this temperatures range, the outer sphere mechanism (OS) dominates relaxivity. By increasing the temperature, the water exchange accelerates, and the IS contribution increases gradually [21]. After the maximum around 330 K, r_1 decreased due to the decrease with the temperature of IS and OS. On the other hand, the increasing trend of r_1 with temperature shown by GdL3 was been observed previously. Based on these data, solid hypotheses cannot be advanced, but this behaviour seems to be associated with an instability of the complex, already observed in the region at basic pH (Figure 3C).

Table 1. Best-fit parameters obtained from the analysis of the ^{1}H NMRD profiles (298 K), ^{1}H-VT and ^{17}O NMR data.

Parameters	$[GdL1]^{3+}$	$[GdL2]^{3+}$	$[GdL3]^{3+}$	$[GdDOTAM](CF_3SO_3)_3$ [b]
r_1 (mM^{-1} s^{-1})	3.0	3.5	2.5	2.5
Δ^2 (10^{19} s^{-2})	2.0	1.0	3.9	1.7
τ_V (ps)	7.6	10.0	18.0	6.0
τ_R (ps)	120	120	120	80
τ_M (μs)	16.0	9.1	40.0	17.0
ΔH_M (kJ mol^{-1})	50.7	37.4	62.0	49.0
r (Å) [a]	3.0	3.0	3.0	3.1
$A/\hbar$ (10^6 rad s^{-1})	−3.6	−3.4	−3.6	-
q [a]	1	1	1	1
a (Å) [a]	4.2	4.2	4.4	4.3
D (10^{-5} cm^2 s^{-1}) [a]	2.24	2.24	2.24	2.24
E_D (kJ mol^{-1})	−28	−29	−28	−23

[a] Parameters fixed during the fitting procedure. [b] Taken from Reference [9].

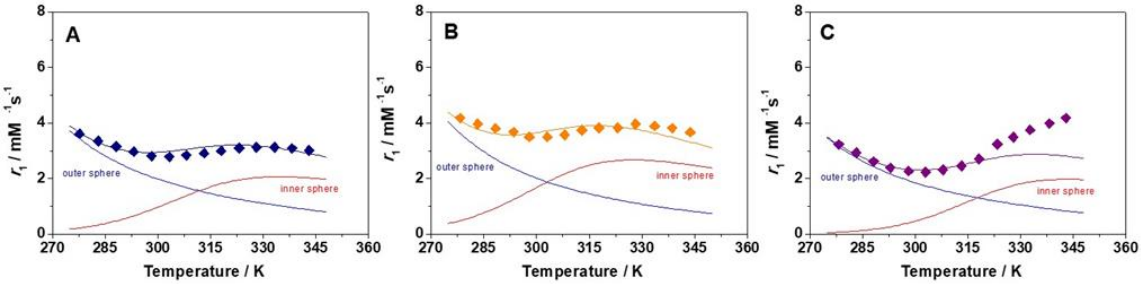

Figure 2. Temperature dependence of the ^{1}H relaxivity at 20 MHz (pH 7) of GdL1 ((**A**) 2.8 mM), GdL2 ((**B**) 2.7 mM), and GdL3 ((**C**) 4.4 mM). The solid lines represent the fits of the data with the parameters reported in Table 1. The dotted lines identify the inner- and outer-sphere contributions.

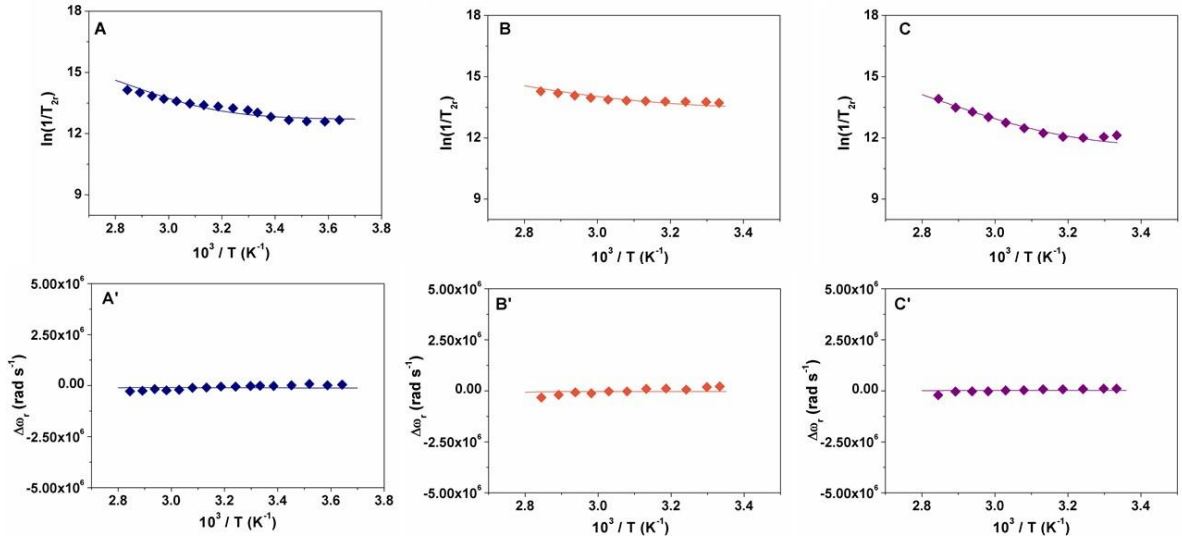

Figure 3. Reduced ^{17}O NMR transverse relaxation rate and ^{17}O NMR chemical shift measured at 67.8 MHz (11.74 T) for GdL1 ((**A**,**A′**) 10.1 mM), GdL2 ((**B**,**B′**) 6.7 mM) and GdL3 ((**C**,**C′**) 24.6 mM). The solid lines represent the fit of the data with the parameters reported in Table 1.

The best direct way to measure k_{ex} is represented by ^{17}O NMR. This technique consists of the measurement of the temperature dependence of the paramagnetic contribution (R_{2p}) to the observed ^{17}O water solvent transverse relaxation rate and chemical shift. This was done at 11.75 T on fairly concentrated aqueous solutions of the complexes at neutral pH. The reduced transverse ^{17}O relaxation

rates ($1/T_{2r}$) increased with increasing temperature over the entire range of values (Figure 3). This indicates the occurrence the slow exchange condition, in agreement with the ^{1}H VT data.

To complete the NMR relaxometric characterization, the ^{1}H nuclear magnetic relaxation dispersion (NMRD) profiles were recorded on approximately 2-mM aqueous solutions of the complexes in the proton Larmor frequency range 0.01–60 MHz (Figure 4). The shape of profiles reproduces closely that typical of low molecular weight Gd(III) complexes, with a plateau at low magnetic fields (0.01–1 MHz), followed by a dispersion in the 1–10 MHz range. However, the relaxivity assumed markedly lower values, indicating that the low exchange rate of the coordinated water significantly reduced the IS contribution. Therefore, r_1 was dominated by the OS contribution, as evidenced by its values at 20 MHz: 3.0, 3.5, and 2.5 mM^{-1} s^{-1} for GdL1, GdL2 and GdL3, respectively (298 K).

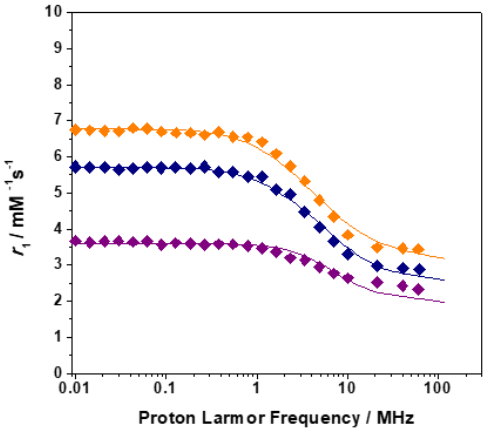

Figure 4. ^{1}H NMRD profiles of at 298 K of GdL1 (blue, 2.4 mM), GdL2 (orange, 2.5 mM) and GdL3 (purple, 4.4 mM). The solid lines were calculated with the parameters reported in Table 1.

The analysis of the ^{1}H and ^{17}O NMR data was performed by using the Solomon–Bloembergen–Morgan (SBM) [22,23] and Freed's equations [24] for the inner- and outer-sphere proton relaxation mechanisms and the Swift–Connick theory for ^{17}O relaxation [25]. The ^{17}O R_2 data depends on several parameters such as the number of inner sphere water molecules (q), their residence lifetime (τ_M), the electronic relaxation times ($T_{1,2e}$), which are described in terms of the square of the zero-field splitting tensor (Δ^2) and the correlation time describing its modulation (τ_V), and the hyperfine Gd–$^{17}O_{water}$ coupling constant ($A/\hbar$). Other relevant parameters are the activation energy of τ_V (E_V) and the activation enthalpy of the water exchange process, ΔH_M.

The best fitting parameters are reported in Table 1. Following a well-established practice, some parameters were fixed at reasonable values due to the large number of parameters that must be considered during the analysis: the hydration number q was fixed at 1; the distance between Gd(III) and the protons of the bound water molecule, r, was fixed at 3.0 Å; D was set at 2.3×10^{-5} cm^2 s^{-1} (at 25 °C); E_V was fixed at 1.0 kJ mol^{-1}. An independent confirmation that these types of complexes are monohydrated was obtained by measuring the luminescence lifetimes of EuL1 in both H_2O and D_2O, (Table S1), and applying established equations to estimate the lanthanide hydration state. A q value of 1.03 was obtained from the experimental data confirming the hypothesis made.

The ^{17}O hyperfine coupling constants ($A/\hbar$) fall within the range typically observed for low molecular weight Gd(III) chelates ($-3.3/-3.6 \times 10^6$ rad s^{-1}) and τ_M values were determined as 16.0 µs for GdL1, 9.1 µs for GdL2 and 40.0 µs in the case of GdL3. The τ_M value for GdL1 was comparable to that reported for other Gd-DOTA-tetraamides [7], about two orders of magnitude longer than for $[Gd(DOTA)]^-$. The strong binding interaction with metal ion of the water molecule in axially-symmetric cationic complexes was reinforced by the presence of electron-withdrawing groups, like the ethyl benzoate functionalities, which reduce the electron density on the amide oxygen donors.

Indeed, the τ_M value of GdL3 was 2.5 times longer than that of GdL1. Conversely, the presence of electron-donating phenylmethoxy groups in the side arms of DOTA-tetraanilide (GdL2) promotes an easier process of water exchange (τ_M = 9.1 μs). The long τ_M values calculated for the complexes were associated with large values of the activation enthalpy (approximately 40–60 kJ mol^{-1}), sensibly greater than those found for anionic and neutral Gd(III) complexes. The electron relaxation parameter Δ^2 was very similar for the three complexes and similar to the values found for related macrocyclic complexes. This suggests the occurrence of similar solution structures for the complexes.

The value of the reorientational correlation time (τ_R) was not accurately determined because the IS contribution in the NMRD profiles was very small. The best results were obtained with the value of 120 (±15) ps, which reflects well the molecular mass of these complexes. On the other hand, by fixing an identical value of r and τ_R to the three complexes, we obtained small differences in the values of the minimum approach distance a between the bulk water and the Gd^{3+} ion.

The set of parameters calculated was quite satisfactory as it not only was consistent with reported values for similar complexes, but it allowed for reproducing well all the experimental data.

2.3. CEST Experiments

An additional evidence of the effect of the aromatic ring substituents on the exchange rate of the coordinated water molecule is provided by the CEST effect measured on the Eu(III) complexes of L1, L2 and L3. The Eu(III) complexes of DOTA tetraamide derivatives are known to possess a slowly exchanging water molecule that yields a CEST peak at about 47 ppm from the resonance of bulk water [18]. Amide protons might also contribute to a CEST effect, but at a very different offset (for instance, −2.5 ppm for the Eu(III)-tetraglycineamide-DOTA (EuDOTAMGly) complex [26]. As shown in Figure 5, the Z-spectrum of EuL1 (pH 7.0, 298 K) shows a fairly well-defined CEST peak. The CEST peak appears as a weak shoulder on the direct saturation peak for EuL2, while it is barely observable as an asymmetry of the direct saturation peak for EuL3. The Z-spectra were fitted to a two-site exchange model according to available theory [20], yielding k_{ex} = 36 × 10^3 Hz, τ_M = 28 μs and Δω = 43 ppm for EuL1, and k_{ex} = 67 × 10^3 Hz, τ_M = 15 μs and Δω = 48 ppm for EuL2. Although the Z-spectrum of EuL3 could not be fitted because of the poor definition of the CEST peak, τ_M could be guessed to be much larger than 28 μs. The values of τ_M did not match exactly those of the corresponding Gd(III) complexes (Table 1), most likely because of the fact that the molar ratios of SAP and TSAP isomers were significantly different between the Eu(III) and Gd(III) complexes, and because of fine structural differences. However, the change of τ_M as a function of the aromatic substituent was the same for the Eu(III) and Gd(III) complexes, confirming the electronic effects of the aromatic ring substituents on water exchange.

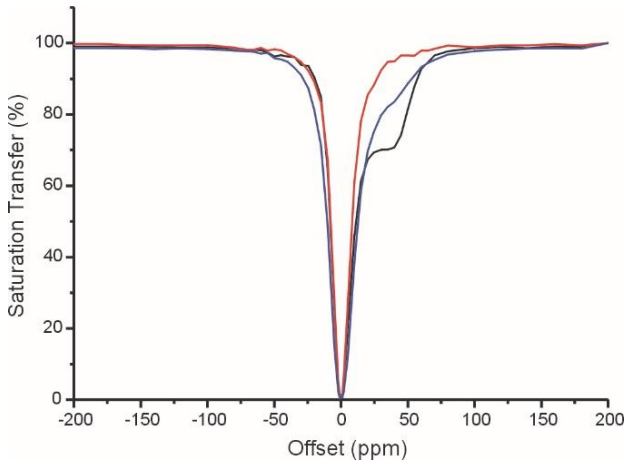

Figure 5. Z-spectra at pH 7, 300 K (irradiation time 2 s at 37 μT): $[EuL1]^{3+}$ 5.3 mM (black), $[EuL2]^{3+}$ 4.9 mM (blue) and $[EuL3]^{3+}$ 4.0 mM (red).

3. Materials and Methods

3.1. General

All chemicals were purchased from Sigma–Aldrich (Saint Louis, MO, USA) or Alfa Aesar (Haverhill, MA, USA) unless otherwise stated and were used without further purification. The ^{1}H and ^{13}C NMR spectra were recorded using a Bruker Avance III 500 MHz (11.4 T) spectrometer (Bruker, Billerica, MA, USA) equipped with 5 mm probe and BVT-3000 temperature control unit. Chemical shifts were reported relative to tetramethylsilane (TMS) and were referenced using the residual proton solvent resonances. The HPLC analyses and mass spectra were performed on a Waters HPLC-MS system (Waters, Milford, CT, USA) equipped with a Waters 1525 binary pump. Analytical measurements were carried out on a Waters Atlantis RPC18 column (T3 5 μm 4.6 × 150 mm) with the following method: A (TFA 0.1% in H_2O); B (MeOH); flow 1 mL/min; 0–3 min: 30% A, 3–17 min: from 30 to 100% B, 17–19 min 100% B, 19–20 min from 100 to 30% B. Electrospray ionization mass spectra (ESI MS) were recorded using a SQD 3100 Mass Detector (Waters, Milford, CT, USA), operating in the positive or negative ion mode, with 1% *v*/*v* formic acid in methanol as the carrier solvent.

3.2. Synthesis of 2-Bromo-N-phenyl-acetamide

Five-hundred milligrams (5.38 mmol) of aniline were dissolved in CH_2Cl_2 (7 mL) and 14 mL NaOH 1 M were added to obtain a biphasic solution. Bromoacetyl bromide (701 μL, 8.07 mmol) was added dropwise and the reaction was left stirring overnight. The two phases were separated, the organic phase washed with H_2O and the product was obtained in pure form (912 mg, 80% yield). ^{1}H NMR (500 MHz, $CDCl_3$, 300 K): δ (ppm) = 4.03 (2, s, CH_2Br), 7.17 (2, t, *J* = 7.4 Hz, *p*-Ph), 7.36 (2, m, *m*-Ph), 7.53 (2, d, *J* = 8.0 Hz, *o*-Ph) 8.11 (1, brs, NH); ^{13}C NMR (125 MHz, $CDCl_3$, 300 K): δ 29.5 ($\underline{C}H_2Br$), 120.0 (*o*-Ph), 125.2 (*p*-Ph), 129.1 (*m*-Ph), 136.9 (Ph–NH) 163.3 ($\underline{C}ONH$); ESI-MS (*m*/*z*): found 213.36 $[M + H]^+$ (calc: C_8H_8BrNO 212.98).

3.3. Synthesis of 2-Bromo-N-(4-methoxyphenyl)-acetamide

Following the same procedure described above, starting from 4-methoxyaniline (500 mg, 4.06 mmol) and bromoacetyl bromide (6.10 mmol), the compound was obtained in 75% yield (738 mg). ^{1}H NMR (500 MHz, $CDCl_3$, 300 K): δ (ppm) = 3.80 (3, s, CH_3O-), 4.01 (2, s, CH_2Br), 6.88 (2, d, *J* = 9.0 Hz, *m*-Ph), 7.42 (2, d, *J* = 9.0 Hz, *o*-Ph), 8.07 (1, brs, NH); ^{13}C NMR (125 MHz, $CDCl_3$, 300 K): δ (ppm) = 29.5 ($\underline{C}H_2Br$), 55.5 ($\underline{C}H_3O$–), 114.3 (*m*-Ph), 122.0 (*o*-Ph), 129.9 (Ph), 157.1 ($\underline{Ph}$–OCH_3), 163.3 ($\underline{C}ONH$); ESI-MS (*m*/*z*): found 243.37 $[M + H]^+$ (calc: $C_9H_{10}BrNO_2$ 242.99).

3.4. Synthesis of 2-Bromo-N-(ethylbenzoate)-acetamide

Following the same procedure described above, starting from ethyl 4-aminobenzoate (500 mg, 3.03 mmol) and bromoacetyl bromide (4.54 mmol), the compound was obtained in 78% yield (676 mg). ^{1}H (500 MHz, $CDCl_3$, 300 K): δ 1.41 (3, t, *J* = 7.1 Hz, $C\underline{H_3}CH_2O$–), 4.05 (2, s, $C\underline{H_2}Br$), 4.39 (2, q, *J* = 7.1 Hz, $CH_3C\underline{H_2}O$–), 7.65 (2, d, *J* = 8.7 Hz, *o*-Ph), 8.06 (2, d, *J* = 8.7 Hz, *m*-Ph), 8.29 (1, brs, NH); ^{13}C NMR (125 MHz, $CDCl_3$, 300 K): δ 14.3 ($\underline{C}H_3CH_2O$–), 29.3 ($\underline{C}H_2Br$), 61.0 ($CH_3\underline{C}H_2O$–), 119.0 (*o*-Ph), 127.0 (*p*-Ph), 129.8 (Ph) 130.8 (*m*-Ph), 140.9 (Ph–NH), 163.5 ($\underline{C}ONH$), 165.9 (Ph–$\underline{C}OO$–); ESI-MS (*m*/*z*): found 287.03 $[M + H]^+$ (calc: $C_{12}H_{14}BrNO_3$ 286.12).

3.5. Synthesis of 1,4,7,10-Tetrakis((phenyl)carbamoylmethyl)-1,4,7,10-tetraazacyclododecane (DOTAMPh (L1))

2-bromo-*N*-phenyl-acetamide (500 mg, 2.36 mmol), 1,4,7,10-tetraazacyclododecane (90 mg, 0.52 mmol) and K_2CO_3 (325 mg, 2.36 mmol) were dissolved in 15 mL ACN, at reflux for 24 h. After the reaction was complete, the mixture was filtrated, the solid was washed 3 times with H_2O and dried in vacuum to give pure L1 ligand (997 mg, 60% yield). Analytical HPLC: t_r = 14.65 min. ^{1}H NMR (500 MHz, DMSO, 300 K): δ (ppm) 2.91 (brs, H macrocycle), 3.32 (brs, $C\underline{H_2}CO$), 7.06 (4, t, *J* = 7.4 Hz, *p*-Ph),

7.27 (8, m, *m*-Ph), 7.61 (8, d, *J* = 8.0 Hz, *o*-Ph), 10.01 (4, s, NH); ^{13}C NMR (125 MHz, DMSO, 300 K): δ (ppm) 52.6 (C macrocycle), 57.9 (CH_2CO), 119.3 (*o*-Ph), 123.2 (*p*-PH), 128.5 (*m*-Ph), 138.6 (Ph–NH), 169.7 (CONH); ESI-MS (*m*/*z*): found 705.65 $[M + H]^+$ (calc: $C_{40}H_{48}N_8O_4$ 704.38).

3.6. Synthesis of 1,4,7,10-Tetrakis-((4-methoxyfenil)-carbamoylmethyl)-1,4,7,10-tetraazacyclododecane (DOTAM^{MeOPh} (L2))

2-bromo-*N*-(methoxyphenyl)-acetamide (500 mg, 2.06 mmol), 1,4,7,10-tetraazacyclododecane (79 mg, 0.46 mmol) and K_2CO_3 (284 mg, 2.06 mmol) were dissolved in 15 mL ACN, at reflux for 24 h. After the reaction was complete, the mixture was filtrated, the solid was washed 3 times with H_2O and dried in vacuum to give pure L2 ligand (1.26 g, 60% yield). Analitycal HPLC: t_r = 13.99 min. ^{1}H NMR (500 MHz, DMSO, 300 K): δ 3.19 (12, brs, H macrocycle), 3.25 (brs, CH_2CO), 3.72 (s, CH_3O–), 6.83 (8, d, 8.9, *m*-Ph), 7.53 (8, d, 8.9, *o*-Ph), 10.08 (4, brs, NH); ^{13}C NMR (125 MHz, DMSO, 300 K): δ 51.0 (C macrocycle), 55.1 (CH_3O-), 58.0 (CH_2CO), 113.7 (*m*-Ph), 121.1 (*o*-Ph), 131.8 (Ph–NH), 155.3 (Ph–OCH_3), 169.3 (CONH); ESI-MS (*m*/*z*): found 825.44 $[M + H]^+$ (calc: $C_{44}H_{56}N_8O_8$ 824.42).

3.7. Synthesis of 1,4,7,10-Tetrakis((4-ethylbenzoate)-carbamoylmethyl)-1,4,7,10-tetraazacyclododecane (DOTAM^{EtBenz} (L3))

2-bromo-*N*-(ethylbenzoate)-acetamide (500 mg, 1.75 mmol), 1,4,7,10-tetraazacyclododecane (67 mg, 0.39 mmol) and K_2CO_3 (241 mg, 1.75 mmol) were dissolved in 15 mL ACN, at reflux for 24 h. After the reaction was complete, the mixture was filtrated, the solid was washed 3 times with H_2O and dried in vacuum to give pure L3 ligand (1.08 g, 62% yield). Analytical HPLC: t_r = 14.83 min. ^{1}H (500 MHz, DMSO, 300 K): δ 1.29 (12, t, 7.1, CH_3CH_2O–); 2.87 (brs, H macrocycle); 3.32 (brs, CH_2CO); 4.26 (8, q, 7.1, CH_3CH_2O–); 7.68 (8, d, 8.7, *o*-Ph); 7.81 (8, d, 8.7, *m*-Ph); 10.24 (4, brs, NH); ^{13}C (125 MHz, DMSO, 300 K): δ 14.1 (CH_3CH_2O–); 52.3 (C macrocycle); 57.9 (CH_2CO); 60.3 (CH_3CH_2O–); 118.6 (*o*-Ph); 124.2 (*p*-Ph); 130.0 (*m*-Ph); 142.9 (Ph–NH); 165.2 (Ph–COO–); 170.2 (CONH); ESI-MS (*m*/*z*): found 993.43 $[M + H]^+$ (calc: $C_{52}H_{64}N_8O_{12}$ 992.46).

3.8. General Procedure for Preparation of Ln(III) Complexes

Fifty milligrams of ligand were dissolved in a 1:1 (*v*/*v*) DMF/H_2O solution (10 mL) at 50 °C, and then $Ln(CF_3SO_3)_3$ (Ln = Gd(III), Eu (III) or Yb (III)) were added. After 36 h, formation of the complex was checked at HPLC/MS. The possible excess metal ion was then precipitated as $Ln(OH)_3$ at pH 10 and filtered. Finally, in order to increase the solubility of the complex in water, the counter-ion $(CF_3SO_3)^-$ was exchanged with Cl^- using a Dowex 1–8(Cl) strong anion resin.

GdL1: Analytical HPLC: t_r = 12.02 min. ESI-MS (*m*/*z*): 863.41 $[M + H]^+$, 430.78 $[M + 2H]^{2+}$, 976.53 [M + TFA]$^+$, (calc: $GdC_{40}H_{48}N_8O_4$ 862.30).

GdL2: Analytical HPLC: t_r = 12.6 min. ESI-MS (*m*/*z*): 983.32 $[M + H]^+$, 1094.29 [M + TFA]$^+$, (calc: $GdC_{44}H_{56}N_8O_8$ 982.35).

GdL3: Analytical HPLC: t_r = 13.55 min. ESI-MS (*m*/*z*): 1151.43 $[M + H]^+$, 754.64 $[M + 2H]^{2+}$, 1261.01 [M + TFA]$^+$, (calc: $GdC_{52}H_{64}N_8O_{12}$ 1150.39).

EuL1: Analytical HPLC: t_r = 11.06 min. ESI-MS (*m*/*z*): 858.54 $[M + H]^+$, 428.48 $[M + 2H]^{2+}$, 969.53 [M + TFA]$^+$, (calc: $EuC_{40}H_{48}N_8O_4$ 857.30).

EuL2: Analytical HPLC: t_r = 12.65 min. ESI-MS (*m*/*z*): 978.54 $[M + H]^+$, 1092.37 [M + TFA]$^+$, (calc: $EuC_{44}H_{56}N_8O_8$ 977.34).

EuL3: Analytical HPLC: t_r = 14.07 min. ESI-MS (*m*/*z*): 1146.47 $[M + H]^+$, (calc: $EuC_{52}H_{64}N_8O_{12}$ 1145.39).

YbL1: Analytical HPLC: t_r = 10.88 min. ESI-MS (*m*/*z*): 879.58 $[M + H]^+$, 438.18 $[M + 2H]^{2+}$ (calc: $YbC_{40}H_{48}N_8O_4$ 878.32).

3.9. ^{1}H Relaxometric Measurements and ^{1}H NMRD Profiles

The water proton relaxation measurements and the ^{1}H NMRD profile were performed with a Stelar Smart Tracer loop relaxometer (Stelar, Pavia, Italy), in a range between 0.01 to 10 MHz (0.00024 to 0.25 T), and with a Stelar Spinmaster console connected to a WP-80 (80 MHz, 2 T). The ^{1}H T_1 relaxation time were acquired with a standard inversion recovery experiment by a 90° pulse width of 3.5 µs. The temperature was set with a Stelar VCT-thermocouple heater. The complexes were prepared in Milli-Q water and their concentrations were determined by measuring the bulk susceptibility shift of the ^{t}BuOH signal between the samples and a standard reference.

3.10. VT ^{17}O Relaxation Measurements

Variable temperature ^{17}O NMR measurements were carried out with a Bruker Advance III 500 MHz (11.4 T) spectrometer (Bruker, Billerica, MA, USA) equipped with a 5 mm probe and BVT-3000 temperature control unit. The complexes were prepared in a water solution enriched with ^{17}O isotope. The transverse relaxation rates (R_2) were calculated from the half height width of the signal.

3.11. Luminescence Measurements

The luminescence lifetime measurements were carried out on a Fluorolog fluorometer using photomultiplier tube, electronics and software supplied by Horiba Jobin Yvon (Kyoto, Japan). The lifetime measurement was carried out using the Data Station v2.5 software (Horiba Jobin Yvon). The subsequent data analysis was performed using the DAS6 v6.4 software (Horiba Jobin Yvon).

3.12. Chemical Exchange Saturation Transfer (CEST)

Z-spectra of Eu(III) complexes were recorded at 11.4 T (corresponding to 500 MHz proton Larmor frequency) by means of a Bruker Avance III NMR spectrometer (Bruker, Billerica, MA, USA) equipped with a triple resonance 5-mm Z-gradient inverse probe. The paramagnetic complexes were dissolved in a 5–10 mM concentration of H_2O:D_2O 90:10 to achieve the field-frequency lock. Z-spectra were acquired by means of the noediff.2 pulse program, with an irradiation time of 2 s at 18–37 µT. The water signal was placed at the centre of the spectrum and the irradiation offset covered the range between +100,000 and −100,000 Hz relative to the water resonance. Typically, 50 data points were collected to obtain a Z-spectrum. Data were processed with the Bruker topspin 3.0.b29 software package. The percent saturation transfer (ST%) was calculated by the following formula:

$$\mathrm{ST\%} = 100 \times (1 - I/I_0) \quad (1)$$

where I is the intensity of the water signal at a given irradiation frequency and I_0 is the maximum intensity of the water signal (off-resonance pre-saturation). Z-spectra were fitted to the Bloch equations modified to obtain water exchange rates according to a two-sites exchange model [27] to obtain the water exchange kinetic constant k_{ex} and the coordinated water resonance offset $\Delta\omega$.

4. Conclusions

Three DOTAM-like ligands were synthesized featuring as amide *N*-substituents phenyl, *p*-methoxyphenyl and *p*-ethylbenzoate groups. The electronic character of the substituents on the *para*-position of the aromatic ring were shown to markedly influence the properties of the corresponding Ln(III) complexes (Ln = Gd and Eu). A detailed ^{1}H and ^{17}O NMR relaxometric study on the Gd(III) complexes allowed to assess that the exchange rate of the coordinated water molecule was five times faster for GdL2 than for GdL3. This was attributed to the electron donating effect of the phenylmethoxy group in GdL2 and to the presence of the electron withdrawing ethylbenzoate group in GdL3. An evaluation of the CEST behaviour of the Eu(III) complexes highlighted a variation of τ_M as a function of the nature of the aromatic substituent identical to that of the Gd(III) complexes.

These results clearly show that the electronic effects of substituents on the pendant arms can modulate k_{ex} in macrocyclic Ln-chelates. This is relevant because the modulation of the coordinated water exchange dynamics in Ln(III) complexes is a feature of paramount importance for the development and optimization of both Gd-based and paraCEST MRI probes.

Supplementary Materials: The following are available online at http://www.mdpi.com/2304-6740/7/4/43/s1, Equations Used for the Analysis of ^{17}O NMR and NMRD Data, Table S1: Emission lifetimes and hydration numbers determined for $[EuL1]^{3+}$ complex.

Author Contributions: Conceptualization: L.T., M.B.; Investigation: L.L., F.C.; Writing-Original Draft Preparation: V.L., F.C., L.T.; Supervision: F.C., L.T., M.B.; Methodology: V.L., G.D., L.T.; Formal Analysis: G.D., M.B.; Writing-Review & Editing: G.D., M.B.; Funding Acquisition: M.B.

Funding: This research was supported by the Università del Piemonte Orientale (Ricerca locale 2016).

Acknowledgments: This study was performed in the framework of COST Action CA15209 "*European Network on NMR Relaxometry*" and the Consorzio Interuniversitario di Ricerca in Chimica dei Metalli nei Sistemi Biologici (CIRCMSB).

Conflicts of Interest: The authors declare no conflict of interest.

References

1. Stasiuk, G.J.; Long, N.J. The ubiquitous DOTA and its derivatives: The impact of 1,4,7,10-tetraazacyclododecane-1,4,7,10-tetraacetic acid on biomedical imaging. *Chem. Commun.* **2013**, *49*, 2732–2746. [CrossRef] [PubMed]
2. Lattuada, L.; Barge, A.; Cravotto, G.; Giovenzana, G.B.; Tei, L. The synthesis and application of polyamino polycarboxylic bifunctional chelating agents. *Chem. Soc. Rev.* **2011**, *40*, 3019–3049. [CrossRef]
3. Brücher, E.; Tircsó, G.; Baranyai, Z.; Kovács, Z.; Sherry, A. Chapter 4: Of the Chemistry of Contrast Agents in Medical Magnetic Resonance Imaging. In *Stability and Toxicity of Contrast Agents*, 2nd ed.; Helm, L., Tóth, É., Merbach, A.E., Eds.; John Wiley & Sons: New York, NY, USA, 2013.
4. Caravan, P.; Ellison, J.J.; McMurry, T.J.; Lauffer, R.B. Gadolinium(III) Chelates as MRI contrast agents: Structure, dynamics, and applications. *Chem. Rev.* **1999**, *99*, 2293–2352. [CrossRef]
5. Wahsner, J.; Gale, E.M.; Rodríguez-Rodríguez, A.; Caravan, P. Chemistry of MRI Contrast Agents: Current Challenges and New Frontiers. *Chem. Rev.* **2018**. [CrossRef]
6. Heffern, M.C.; Matosziuk, L.M.; Meade, T.J. Lanthanide Probes for Bioresponsive Imaging. *Chem. Rev.* **2014**, *114*, 4496–4539. [CrossRef]
7. Aime, S.; Barge, A.; Bruce, J.I.; Botta, M.; Howard, J.A.K.; Moloney, J.M.; Parker, D.; de Sousa, A.S.; Woods, M. NMR, Relaxometric, and Structural Studies of the Hydration and Exchange Dynamics of Cationic Lanthanide Complexes of Macrocyclic Tetraamide Ligands. *J. Am. Chem. Soc.* **1999**, *121*, 5762–5771. [CrossRef]
8. Aime, S.; Barge, A.; Batsanov, A.S.; Botta, M.; Delli Castelli, D.; Fedeli, F.; Mortillaro, A.; Parker, D.; Puschmannd, H. Controlling the variation of axial water exchange rates in macrocyclic lanthanide(III) complexes. *Chem. Commun.* **2002**, *10*, 1120–1121. [CrossRef]
9. Thompson, A.L.; Parker, D.; Fulton, D.A.; Howard, J.A.K.; Pandya, S.U.; Puschmann, H.; Senanayake, K.; Stenson, P.A.; Badari, A.; Botta, M.; et al. On the role of the counter-ion in defining water structure and dynamics: Order, structure and dynamics in hydrophilic and hydrophobic gadolinium salt complexes. *Dalton Trans.* **2006**, *47*, 5605–5616. [CrossRef]
10. Aime, S.; Barge, A.; Botta, M.; De Sousa, A.S.; Parker, D. Direct NMR Spectroscopic Observation of a Lanthanide-Coordinated Water Molecule whose Exchange Rate Is Dependent on the Conformation of the Complexes. *Angew. Chem. Int. Ed.* **1998**, *37*, 2673–2675. [CrossRef]
11. Aime, S.; Barge, A.; Botta, M.; Parker, D.; De Sousa, A.S. Prototropic vs Whole Water Exchange Contributions to the Solvent Relaxation Enhancement in the Aqueous Solution of a Cationic Gd^{3+} Macrocyclic Complex. *J. Am. Chem. Soc.* **1997**, *119*, 4767–4768. [CrossRef]
12. Woods, M.; Pasha, A.; Zhao, P.; Tircso, G.; Chowdhury, S.; Kiefer, G.; Woessner, D.E.; Sherry, A.D. Investigations into whole water, prototropic and amide proton exchange in lanthanide(III) DOTA-tetraamide chelates. *Dalton Trans.* **2011**, *40*, 6759–6764. [CrossRef]

13. Zhang, S.; Winter, P.; Wu, K.; Sherry, A.D. A Novel Europium(III)-Based MRI Contrast Agent. *J. Am. Chem. Soc.* **2001**, *123*, 1517–1518. [CrossRef]
14. Zhang, S.; Wu, K.; Biewer, M.C.; Sherry, A.D. ^{1}H and ^{17}O NMR detection of a lanthanide-bound water molecule at ambient temperatures in pure water as solvent. *Inorg. Chem.* **2001**, *40*, 4284–4290. [CrossRef] [PubMed]
15. McVicar, N.; Li, A.X.; Suchy, M.; Hudson, R.H.E.; Menon, R.S.; Bartha, R. Simultaneous in vivo pH and temperature mapping using a PARACEST-MRI contrast agent. *Magn. Reson. Med.* **2013**, *70*, 1016–1025. [CrossRef]
16. Li, X.; Wojciechowski, F.; Suchy, M.; Jones, C.K.; Hudson, R.H.E.; Merton, R.S.; Bartha, R. A sensitive PARACEST contrast agent for temperature MRI: Eu^{3+}DOTAM-Glycine (Gly)-Phenylalanine (Phe). *Magn. Reson. Med.* **2008**, *59*, 374–381. [CrossRef]
17. Milne, M.; Lewis, M.; McVicar, N.; Suchy, M.; Bartha, R.; Hudson, R.H.E. MRI ParaCEST agents that improve amide based pH measurements by limiting inner sphere water T_2 exchange. *RSC Adv.* **2014**, *4*, 1666–1674. [CrossRef]
18. Ratnakar, S.J.; Woods, M.; Lubag, A.J.M.; Kov´acs, Z.; Sherry, A.D. Modulation of Water Exchange in Europium(III) DOTA-Tetraamide Complexes via Electronic Substituent Effects. *J. Am. Chem. Soc.* **2008**, *130*, 6–7. [CrossRef]
19. Remya, G.S.; Suresh, C.H. Quantification and classification of substituent effects in organic chemistry: A theoretical molecular electrostatic potential study. *Phys. Chem. Chem. Phys.* **2016**, *18*, 20615–20626. [CrossRef]
20. Martinelli, J.; Balali-Mood, B.; Panizzo, R.; Lythgoe, M.F.; White, A.J.P.; Ferretti, P.; Steinke, J.H.G.; Vilar, R. Coordination chemistry of amide-functionalised tetraazamacrocycles: Structural, relaxometric and cytotoxicity studies. *Dalton Trans.* **2010**, *39*, 10056–10067. [CrossRef]
21. Helm, L.; Morrow, J.R.; Bond, C.J.; Carniato, F.; Botta, M.; Braun, M.; Baranyai, Z.; Pujales-Paradela, R.; Regueiro-Figueroa, M.; Esteban-Gómez, D.; et al. *Contrast Agents for MRI: Experimental Methods*; Pierre, V.C., Allen, M.J., Eds.; The Royal Society of Chemistry: London, UK, 2017; pp. 121–242.
22. Solomon, I.; Bloembergen, N. Nuclear Magnetic Interactions in the HF Molecule. *J. Chem. Phys.* **1956**, *25*, 261–266. [CrossRef]
23. Bloembergen, N.; Morgan, L.O. Proton relaxation times in paramagnetic solutions. Effects of electron spin relaxation. *J. Chem. Phys.* **1961**, *34*, 842–850. [CrossRef]
24. Freed, J.H. Dynamic effect of pair correlation functions on spin relaxation by translational diffusion in liquids. II. Finite jumps and independent t1 processes. *J. Chem. Phys.* **1978**, *69*, 4034–4037. [CrossRef]
25. Swift, T.J.; Connick, R.E.J. NMR-relaxation mechanisms of ^{17}O in aqueous solutions of paramagnetic cations and the lifetime of water molecules in the first coordination sphere. *J. Chem. Phys.* **1962**, *37*, 307–319. [CrossRef]
26. Terreno, E.; Delli Castelli, D.; Cravotto, G.; Milone, L.; Aime, S. Ln(III)-DOTAMGly complexes: A versatile series to assess the determinants of the efficacy of paramagnetic chemical exchange saturation transfer agents for magnetic resonance imaging applications. *Investig. Radiol.* **2004**, *39*, 235–243. [CrossRef]
27. Woessner, D.E.; Zhang, S.; Merritt, M.E.; Sherry, A.D. Numerical solution of the Bloch equations provides insights into the optimum design of PARACEST agents for MRI. *Magn. Reson. Med.* **2005**, *53*, 790–799. [CrossRef] [PubMed]